Journal of Cleaner Production 209 (2019) 927–936

Contents lists available at ScienceDirect

Journal of Cleaner Production

journal homepage: www.elsevier.com/locate/jclepro

Influence of pyrolysis temperature on production of digested sludge biochar and its application for ammonium removal from municipal wastewater

Yao Tang [a], Md Samrat Alam [b], Kurt O. Konhauser [b], Daniel S. Alessi [b], Shengnan Xu [c], WeiJun Tian [d], Yang Liu [e, *]

[a] Department of Civil and Environmental Engineering, 3-133 Markin/CNRL Natural Resources Engineering Facility, University of Alberta, Edmonton, Alberta, T6G 2W2, Canada
[b] Department of Earth and Atmospheric Sciences, University of Alberta, 1-26 Earth Sciences Building, Alberta, T6G 2E3, Canada
[c] Department of Civil and Environmental Engineering, 7-332 Donadeo Innovation Centre for Engineering, University of Alberta, Edmonton, Alberta, T6G 1H9, Canada
[d] College of Environmental Science and Engineering, Ocean University of China, 5 Yushan Rd, Shinan District, Qingdao City, Shandong Province, 266100, China
[e] Department of Civil and Environmental Engineering, 7-263 Donadeo Innovation Centre for Engineering, University of Alberta, Edmonton, Alberta, T6G 1H9, Canada

ARTICLE INFO

Article history:
Received 29 May 2018
Received in revised form
24 October 2018
Accepted 25 October 2018
Available online 30 October 2018

Keywords:
Ammonium
Adsorption
Biochar
Digested sludge
Pyrolysis

ABSTRACT

Water contamination by ammonium (NH_4^+) can present considerable risks to natural ecosystems. This work evaluates the potential application of biochar, produced from the pyrolysis of digested sludge, to remove ammonium from water. Anaerobic digester sludge was collected from a municipal wastewater treatment plant in Alberta, Canada, and individual biochars were produced at 50 °C temperature increments between 350 °C and 550 °C. The chemical characteristics of the resulting biochars were determined using elemental analysis, scanning electron microscopy (SEM), BET surface area analysis, and Fourier transform infrared spectroscopy (FTIR). Our findings demonstrate that the biochar yield decreased with increasing pyrolysis temperature, and biochar produced at 450 °C (BC450) had the highest ammonium removal capacity due to its higher surface area and functional group density. The Langmuir isotherm best described the observed ammonium removal capacity by the biochars, indicating that monolayer chemical adsorption may be the dominating mechanism. Biochar ammonium removal capacity was 1.2 mg NH_4–N per gram of biochar in municipal wastewater, which is lower than that observed in parallel experiments using a synthetic ammonium solution (1.4 mg NH_4^+-N/g biochar). This phenomenon is likely due to competition between ammonia and other containments for sorption to biochar surface sites. Our results demonstrate for the first time ever that biochar produced from digester sludge is a promising adsorbent for ammonium removal from municipal wastewater.

1. Introduction

Ammonium (NH_4^+) is a soluble pollutant in water systems, influencing potability and causing eutrophication through its role as an oxygen sink during nitrification (Li and Liu, 2009; Yang et al., 2007), while its equilibrium gas phase, ammonia (NH_3), is a potential threat to fish through protein metabolism inhibition (Stuart et al., 2010). Adsorption by various adsorbents (e.g., zeolites, activated carbon and silicates) has been reported to be a promising approach to remove ammonium from water. For instance, the adsorption capability of zeolites was measured as 1.4 mg/g and that of NaOH treated activated carbon to be 2.89 mg/g (Hina et al., 2015; Vu et al., 2018), while the maximum adsorption amount of NH_3 in the micropores of nanostructured silica materials could reach 47.6 mg/g (Roque-Malherbe et al., 2008).

Biochar, as an emerging "cleaner" substitute for activated carbon due to its lower pyrolysis temperature and production cost, is attracting interest with regards to its application in soil remediation (Alam et al., 2018; Kim et al., 2018; Yang et al., 2018). Recent studies have demonstrated that biochar produced from solid

* Corresponding author.
E-mail address: yang.liu@ualberta.ca (Y. Liu).

https://doi.org/10.1016/j.jclepro.2018.10.268
0959-6526/

wastes can be efficient adsorbents at removing metal and organic contaminants from water (e.g., (Inyang et al., 2012; Mohan et al., 2014; Vithanage et al., 2015)). In particular, organic waste materials, such as wood chips (Veksha et al., 2014), coconut shells (Cazetta et al., 2011), wheat straw (Xu et al., 2016) and bamboo (Fan et al., 2010), as well as inorganic cellular materials, such as coal cinder (Wang et al., 2016), can be converted to biochar through pyrolysis (Bridle and Pritchard, 2004; Hospido et al., 2005; Strezov and Evans, 2009). During pyrolysis, the high organic content of such waste is transformed and fixed at a stable carbon phase. Previous studies on the sludge-derived biochar activation process revealed that the raw material and the pyrolysis temperature are the main factors influencing biochar quality and quantity (Smith et al., 2009; Alam et al., 2018). The thermal decomposition of sludge material under high temperature leads to transport and phase-out of non-carbon elements, such as volatile compounds (Carey et al., 2015), resulting in the bonding of liberated carbon atoms as elementary graphitic crystallites (Smith et al., 2009). The interstices between the crystallites propagate a rudimentary porous structure, increasing the porosity and enhancing the adsorption properties of the resulting biochar (Smith et al., 2009).

Anaerobic digester sludge, which is generated as by-product at municipal wastewater treatment facilities, is often disposed of in landfills or by incineration (Lu et al., 2013), or used for land application after sufficient treatment (Bright and Healey, 2003). However, organic matter and nutrients enriched in these biosolids can be recovered and converted into value-added products, such as biochar, thereby avoiding the environmental and economic costs of disposal.

Digested sludge-derived biochars have been found to effectively adsorb numerous contaminants of environmental concern (Paz-Ferreiro et al., 2018), such as Pb, Cr and As (Jin et al., 2014; Zhou et al., 2015), and numerous types of small and large organics from wastewater systems (Kacan, 2016; Shi et al., 2014; Silva et al., 2016; Yao et al., 2013). Digested sludge can be heated at high temperatures to form biochars that have high porosity (Jindarom et al., 2007), ion exchange capacity, as well as various surface functional groups that can facilitate surface chemical reactions (Chen et al., 2002). Biochar has been studied to remove aqueous ammonium as well (Hou et al., 2016; Shin et al., 2018; Zhang et al., 2017) with the adsorption strength varying amongst biochars produced from different feedstocks and pyrolysis temperatures (e.g., 15.8 mg/g for cotton stalk-biochar and 0.52 mg/g for pine biochar) (Gao et al., 2015; Hina et al., 2015). As far as we are aware, only two studies (Carey et al., 2015; Li et al., 2018) reported the application of digested sludge-derived biochar to remove ammonium from aqueous solution. However, the link between pyrolysis temperatures of biochar and their effects on ammonium sorption is still unclear.

In this study, we hypothesized that digested sludge-derived biochars can be used as an alternative to conventional sorbents in water treatment, particularly considering the competition between ammonium and other contaminants that are frequently found in municipal wastewater. We evaluated and compared for the adsorption capacity of digested sludge-derived biochars at removing ammonium from aqueous solution and from municipal wastewater. Different pyrolysis temperatures were used to convert the sludge into various biochar products. The adsorption processes were then evaluated using isotherm and kinetics models.

2. Materials and methods

2.1. Preparation of digested sludge

Anaerobic digester sludge was collected from a biological nutrient removal (BNR) (operated according to the Anaerobic-Anoxic-Aerobic process) Wastewater Treatment Plant (Goldbar WWTP) in Edmonton, Alberta, Canada. The sludge sample was air-dried inside a fume hood at room temperature for one week, then further dried in an oven at 60 °C for 12 h. The dried sludge sample was ground (Homemax HL-2570), passed through a 1 mm sieve which selected the biochars with size below 1 mm, and sealed in a container until use.

2.2. Biochar and solution preparation

The dried and sieved sludge was pyrolyzed to make biochar at 50 °C temperature intervals between 350 and 550 °C in a muffle furnace. To do so, dried, ground, digested sludge (30 g) was weighed and placed in a crucible. The crucible was covered with aluminum foil and put into an 800 cm^3 quartz reactor inside a furnace in an N_2 flow of 25 mL/min. The furnace temperature was raised at a rate of 5 °C/min. Samples of heated sludge (biochar) were obtained from the crucible processed at 350, 400, 450, 500, and 550 °C with 2 h of holding time, cooled in the N_2 environment, weighed, washed with deionized water three times, oven-dried at 60 °C overnight, and then sealed in containers and stored at room temperature until use. Biochar samples were labeled as BC350, BC400, BC450, BC500, and BC550 according to the pyrolysis temperature.

The ability of the biochar produced at different temperatures to adsorb ammonium was tested in both synthetic ammonium solutions and in raw municipal wastewater (primary effluent). The water quality was described in our previous research (Nze et al., 2018) and the average values of major parameters are listed in Table 2. The wastewater and ammonium solutions were autoclaved at 121 °C, filtered through a 0.45 μm membrane, and stored at 4 °C until use.

2.3. Analytical methods

Elements in the digested sludge and the biochar samples were characterized using an elemental analyzer (Flash 2000 HT Plus). All the digested sludge and biochar samples were dried for 12 h in an oven which was set at 60 °C and further cooled down to room temperature in a desiccator before subjected to measurement. Surface area and pore size distribution were determined based on Brunauer-Emmett-Teller (BET) theory by nitrogen (N_2) adsorption/desorption at 77 K using a surface and pore size distribution analyzer (Autosorb Quantachrome 1 MP). Surface morphology changes in biochar samples before, and after, pyrolysis was investigated with a scanning electron microscopy, SEM (Philips/FEI XL30). Surface functional groups were recorded with a Fourier transform infrared (FTIR) spectrometer in the 560–4000 cm^{-1} range (Spectrum 100, PerkinElmer Ltd, Bucks, UK). Biochar production yield percentages at different pyrolysis temperatures were determined with a laboratory scale balance (Denver Instrument. Co., USA) using weight differences between the dried digested sludge and the biochar that formed after pyrolysis. Ammonium concentrations were measured with the Ammonium TNTplus vial test, HR (2–47 mg/L NH_3–N, HACH®, USA) and a benchtop spectrophotometer (DR 3900, HACH®, USA). Biochar pH was determined by adding biochar samples to fresh distilled water with a ratio of 1:5, mixing the samples using a bench top shaker for 30 min at a speed of 110 rpm, and measuring the pH of the supernatant using a pH meter (EXTECH EC500).

2.4. Potentiometric titrations of BC450

Since BC450 was selected as the best biochar for ammonium

removal, to investigate the biochar surface reactivity, BC450 (4 g/L) was suspended in 50 mL nano-pure water, and the mixture was purged with N_2 for 30 min to remove CO_2. Biochar samples were titrated with 0.1 M NaOH from pH 3 to 10 using a Mettler Toledo T50 titrator. This process was then followed by titration with 0.1 M HCl from pH 10 to 3 to test the reversibility of biochar proton binding. The titrator ran dynamically with a 0.5 μM minimum dose and a 0.15 mL maximum dose. Titration data were modelled using FITEQL 4.0 (Herbelin, 1999) to determine the acidity constants and the site concentrations for proton-active functional groups on the biochar surface. A nonelectrostatic surface complexation modeling (NEM SC) approach was used to fit titration data, using the charge balance equation,

$$[C_a - C_b] = [-Q] + \left[H^+\right] + \left[OH^-\right] \quad (1)$$

where C_a and C_b are the concentrations of acid and base, respectively, $[-Q]$ is the negative excess charge, $[H^+]$ is the concentration of protons, and $[OH^-]$ is the concentration of hydroxyl ions. The NEM SC approach considered a discrete number (n) of proton-active surface functional groups in BC 450 represented generally by the equilibrium reaction:

$$\equiv R - L_n - H^0 \leftrightarrow \equiv R - L_n^- + H^+ \quad (2)$$

where ≡R is the macromolecule in BC450 to which surface functional group L_n is attached.

The mass action reaction for the corresponding to the reaction in equation (2) is defined as:

$$K_a = \frac{\left[\equiv R - L_n^-\right] a_{H^+}}{\left[\equiv R - L_n - H^0\right]} \quad (3)$$

where K_a is the protonation constant, $[\equiv R - L_n^-]$ and $[\equiv R - L_n - H^0]$ represent the molar concentration of deprotonated and protonated surface functional groups, respectively, and a_{H^+} is the activity of protons in solution.

To calculate the best fit, we modelled the titration data invoking between one to four (n = 1 to 4) discrete surface functional groups on BC450. The corresponding pK_a values and site concentrations are determined simultaneously. Best-fit models are selected based on the variance parameter, V(Y), calculated in FITEQL, where values of $1 \leq V(Y) \leq 20$ are considered good fits (Herbelin, 1999).

2.5. Ammonium adsorption on biochar samples

Ammonium adsorption on BC350, BC400, BC450, BC500, and BC550 were measured to determine the impact of pyrolysis temperature on biochar ammonium adsorption capacity. Adsorption experiments were carried out in triplicate. Biochar (2.0 g) was added to 200 mL ammonium solution of 45 mg/L NH_4^+–N (the ammonium concentration was selected based on the typical ammonium concentration in centralized WWTP (Nze et al., 2018)) in a 500 mL Erlenmeyer flask, shaken at 100 rpm, and sampled over a series of contact times from 20 to 1560 min at room temperature, and then filtered through a 0.22 μm membrane. The ammonium remaining in solution was analyzed using an ammonium test vial based on the method 10205 HR TNTplus 832 (HACH, Canada). The ammonium removal percentage and the amount of ammonium adsorbed on different biochar samples were calculated based on the difference between initial and final residual concentrations of aqueous ammonium, as described in equations (4) and (5). The ammonium removal percentage is expressed as:

$$\text{ammonium removal percentage } (\%) = \frac{(C_0 - C_t)}{C_0} \times 100\% \quad (4)$$

where C_0 is the initial ammonium concentration (mg/L) in the solution and C_t is the ammonium concentration at time t. The concentration of ammonium adsorbed to each biochar was determined as:

$$Q_t = \frac{V(C_0 - C_t)}{W} \quad (5)$$

where Q_t is the amount of ammonium adsorbed per unit weight of biochar (mg/g) at time t, V is the volume (L) of the ammonium solution, and W is the mass (g) of the adsorbent (Eddy, 2014).

2.6. pH adsorption edge experiments

Ammonium was adsorbed to BC450 as a function of pH to generate a pH adsorption edge. HCl and NaOH were used to adjust 200 mL aliquots of the 45 mg/L NH_4^+ ammonium solution to pH 2, 4, 6, 8, and 10. Biochar (2.0 g) was then mixed into each ammonium solution aliquot in 500 mL Erlenmeyer flasks, to determine the effect of pH on the removal of ammonium from solution by BC450. Ammonium adsorption data were modelled using FITEQL 4.0 to determine the stability constants of ammonium adsorption to BC450 ligands. Site concentrations and pK_a values of BC450 determined by potentiometric titration were used to calculate the binding constants (K) of ammonium adsorption. The NH_4^+- ligand stability constants were determined according to:

$$K_{L_n - NH_4^+} = \frac{\left[R - L_n - NH_4^+\right]}{\left[R - L_n^-\right] a_{NH_4^+}} \quad (6)$$

where the equilibrium constant is $K_{L_n - NH_4^+}$, $[R - L_n - NH_4^+]$ is the concentration of the NH_4^+-biochar surface ligand complex, $[R - L_n^-]$ is the concentration of deprotonated ligands on the biochar surface, and $a_{NH_4^+}$ is the activity of NH_4^+ in solution. The effect of the adsorbate concentration (initial ammonium concentration 2, 4, 6, 8, 10, 20, 40, and 80 mg/L) was also evaluated at solution pH 7.0 and in the presence of 10 g/L of biochar.

2.7. Adsorption isotherms and adsorption kinetics models

The adsorption isotherm experiments were carried out by mixing 2 g of biochar sample with 200 mL synthetic ammonium solution of different initial ammonium concentrations (2, 4, 6, 8, 10, 20, 40, and 80 mg/L) under constant temperature of 20 °C in an incubator shaker set to 100 rpm for 24 h. All experiments were carried out in triplicate. The experimental data were fitted to Langmuir and Freundlich adsorption isotherm models, as described in Equations (7)–(10):

$$q_e = \frac{Q_m K_a C_e}{1 + K_a C_e} \quad (7)$$

where K_a is the Langmuir constant that denotes the energy of adsorption and affinity of the binding sites (L/mg) (Cazetta et al., 2011; Langmuir, 1918), Q_m is the maximum adsorption capacity (mg/g), and C_e is the unit adsorption capacity in the equilibrium (mg/L).

Equation (7) can be transformed to linear models:

$$\frac{1}{q_e} = \frac{1}{Q_m K_a C_e} + \frac{1}{Q_m} \quad (8)$$

$$R_L = \frac{1}{1 + K_a C_e} \quad (9)$$

where R_L is the separation factor (Langmuir, 1918). The Freundlich sorption isotherm can be described by:

$$q_e = K_F C_e^{1/n_F} \quad (10)$$

where K_F and n_F are Freundlich constants (Freundlich, 1906).

Adsorption kinetics were used to investigate the interaction between adsorbent and adsorbate. The Lagergren pseudo-first order model (Lagergren, 1898), and a pseudo-second order model (Blanchard et al., 1984) were used to simulate the adsorption. The Lagergren pseudo-first order kinetics model is expressed in Equations (11) and (12):

$$\frac{dQ}{dt} = k_1(Q_e - Q_t) \quad (11)$$

where, k_1 is the rate constant of first order sorption (l/min); Q_e is the amount of solute sorbed at equilibrium (mg/g); Q_t is amount of solute sorbed by sorbent at time t (mg/g).

Integration of Equation (11) over the boundary conditions $t = 0$ to $t = t$ and $Q_t = 0$ to $Q_t = Q_e$ yields Equation (12) (Ho and McKay, 1999),

$$Q_t = Q_e(1 - \exp(-k_1 t)) \quad (12)$$

The pseudo-second order kinetics model to analyze ammonium adsorption is expressed as:

$$\frac{dQ}{dt} = k_2(Q_e - Q_t)^2 \quad (13)$$

where k_2 is the rate constant of second order sorption (l/min).

Integration of Equation (13) over the boundary conditions $t = 0$ to $t = t$ and $Q_t = 0$ to $Q_t = Q_e$ yields:

$$\frac{1}{Q_e - Q_t} = \frac{1}{Q_e} + k_2 t \quad (14)$$

Equation (14) can be rearranged to Equation (15) to obtain a linear relation (Ho and McKay, 1999).

$$\frac{t}{Q_t} = \frac{1}{k_2 Q_e^2} + k_2 t \quad (15)$$

3. Results and discussion

3.1. Biochar yield and elemental composition

Our results demonstrate that the pyrolysis temperature strongly affected the biochar yield. As shown in Table 1, biochar yield was negatively correlated with the pyrolysis temperature. The biochar weight loss for BC350 was 29.7%, which was lower than for BC550 (42.8%). This may be attributed to the carbonization process associated with thermal decomposition and gasification of the surface groups (Li et al., 2018). The reduction of biochar yield became moderate when temperature increased from 500 °C to 550 °C, indicating the major carbonization process was almost completed (Li et al., 2018). The pH of the resulting biochar steadily increased as the pyrolysis temperature increased, which may be explained by the decomposition and volatilization of organic acids and phenolic substances at higher temperature conditions (Shinogi and Kanri, 2003; Zhang and Wang, 2016).

Analyses of the carbonized biochar indicated that elemental concentrations in the biochar varied with the pyrolysis temperature (Table 1). Between 350 °C and 550 °C, the total nitrogen (N), total hydrogen (H) and total oxygen (O) content decreased as the temperature increased, which may be attributed to the loss of volatile nitrogen species (NH_4^+ and/or NO_3^-) which tend to convert to more stable pyridine compounds at higher temperature. The temperature increase also led to the reduction in the carbon content, in agreement with previous studies (Yu and Zhong, 2006). An increase in the C/N ratio was observed with an increase in pyrolysis temperature, which indicates carbonization and the conversion and gasification of organic nitrogen (Lu et al., 2013). The H/C and O/C ratios represent the degree of aromaticity and polarity, respectively (Table 1). The ratios of H/C (0.04–0.12) and O/C (0.59–0.71) from sludge-based biochars were slightly higher than the values reported by Li (Li et al., 2018), in which H/O ratios were 0.03–0.10 and O/C ratios were 0.16–0.54 from the sludge-derived biochars. This is not an unexpected finding given that both the biosolids source and pyrolysis procedure varied between studies. The dehydration process associated with the increased pyrolysis temperature decreased H/C and O/C values gradually (Table 1). The lower ratios of H/C and O/C also indicate that more aromatic and less hydrophilic biochar surface at higher pyrolysis temperature.

3.2. Optimal pyrolysis temperature

FTIR analyses show systematic changes in surface functional

Table 2
Major parameters of wastewater quality.

	COD	NH_4^+–N	NO_3^--N	NO_2^--N	PO_4^{3-}P
Average Concentration (mg/L)	186	45	0.78	0.07	4.70

Table 1
Physicochemical properties of raw material and biochars under different pyrolysis temperatures (C: Carbon; N: Nitrogen; O: Oxygen; H: Hydrogen).

	Raw	BC 350	BC 400	BC 450	BC 500	BC 550
N (w/w%)	5.9 ± 0.2	3.1 ± 0.1	2.7 ± 0.1	2.6 ± 0.1	2.4 ± 0.1	2.1 ± 0.0
C (w/w%)	34.9 ± 0.8	22.0 ± 0.4	19.4 ± 0.5	18.6 ± 0.4	17.7 ± 0.4	15.7 ± 0.4
O (w/w%)	24.8 ± 0.7	14.9 ± 0.4	12.7 ± 0.4	11.9 ± 0.1	10.9 ± 0.3	9.2 ± 0.3
H (w/w%)	4.2 ± 0.1	1.7 ± 0.1	1.3 ± 0.0	1.0 ± 0.0	0.8 ± 0.0	0.6 ± 0.0
C/N ratio	5.95	7.07	7.14	7.16	7.36	7.60
H/C ratio	0.12	0.08	0.07	0.05	0.04	0.04
O/C ratio	0.71	0.68	0.65	0.64	0.62	0.59
Yield (wt%)		70.3 ± 2.2	64.4 ± 3.6	61.3 ± 3.6	58.4 ± 2.8	57.2 ± 3.0
pH		8.57	8.63	9.47	10.41	10.60

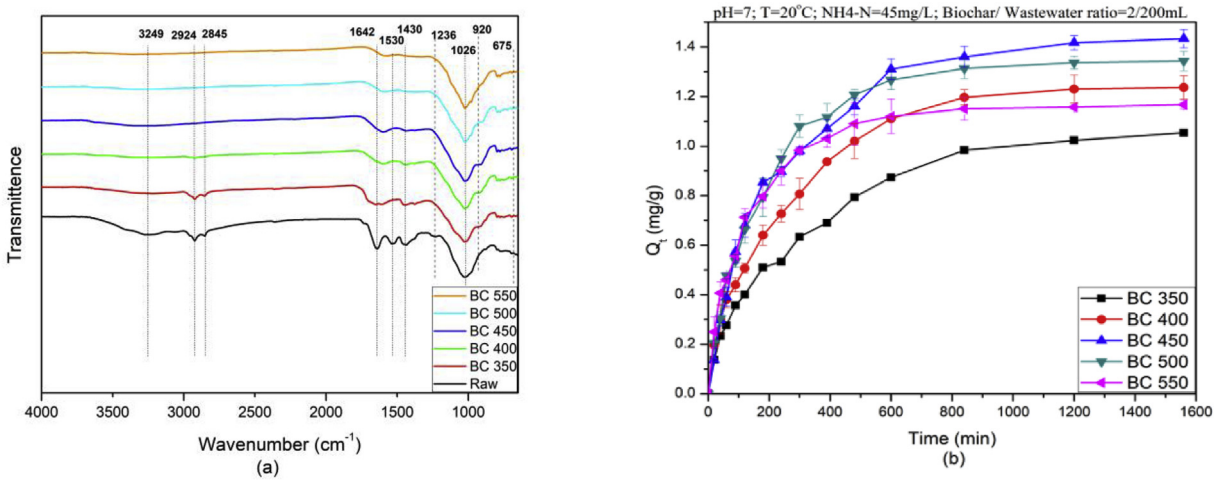

Fig. 1. **(a)** FTIR spectra of digested sludge and biochars produced at different pyrolysis temperatures, and **(b)** ammonia adsorption to biochars produced at different pyrolysis temperatures.

groups of anaerobic digested sludge and their biochar series (Fig. 1(a)). As the temperature increased, gas emission and thermal decomposition of functional groups caused the sludge to carbonize and pores to proliferate. After the pyrolysis temperature reached 400 °C, only small differences in structure and functional groups were observed in biochar samples with further temperature increases. A strong adsorption band was observed from 3700 cm^{-1} to 3200 cm^{-1}, with a peak maximum at 3249 cm^{-1}. This can be assigned to −OH stretching (Peng et al., 2016) and N−H groups comprising proteins. Asymmetric and symmetric stretching in $-CH_3$ groups at 2924 cm^{-1} and 2845 cm^{-1} (Lin et al., 2012), respectively, were present in the sludge and BC350. Organic nitrogen in amines (1240 cm^{-1}) and amides (1530 cm^{-1}) were absent at temperatures higher than 350 °C, and $-CH_3$ groups were unstable at elevated temperatures. The intensity of −OH and $-CH_3$ clearly decreased from BC350 to BC400. Thus, $-CH_3$, −OH, and −NH groups were unstable at elevated temperatures (Jin et al., 2016). The small band at 920 cm^{-1}, apparent from 350 °C to 500 °C, indicates the presence of polysaccharides or phosphodiesters (Gao et al., 2014). On the other hand, aromatic rings (1642 cm^{-1}) and carboxylic acid (1430 cm^{-1}) were quite stable as the pyrolysis temperature increased, supporting crystallization. Clay minerals and quartz (1026 cm^{-1}) remained in the material. Therefore, with the further carbonization process, BC550 had only a few remaining infrared bands, corresponding to aromatic, carbonyl and carboxyl groups (Jiang et al., 2016; Liu et al., 2012), although the aromatic fraction may increase.

The removal of ammonium from synthetic ammonium solutions over time using biochar produced at different pyrolysis temperatures is shown in Fig. 1(b). Biochar produced at 450 °C (BC450) had the highest ammonium adsorption capacity. The maximum ammonium adsorption capacity for BC450 was 1.4 mg/g, similar to that of biochars produced from other feedstocks (e.g., 1.2 mg/g for maple wood biochar) (Wang et al., 2015), but smaller than base modified sludge-derived biochar (5.3 mg/g) (Carey et al., 2015). This pattern is likely due to differing biochar surface properties. Due to the lack of carbonization (Table 1), the biochars pyrolyzed at lower temperatures (BC350, BC400) had relatively lower ammonium adsorption capacities. BC450 showed higher ammonium adsorption capacity as compared to BC350 and BC400, yet BC500 and BC550 adsorbed less ammonium presumably because of the loss of surface functional groups from dehydrogenation, dehydration and condensation (Fig. 1(a)) (Li et al., 2018) and a higher pH (above 10; Table 1) which caused a decline in ammonium adsorption (Vu et al., 2017). Similar results of higher pyrolysis temperature not leading to higher ammonium adsorption capacity were previously observed (Li et al., 2018).

3.3. Characteristics of BC450

3.3.1. BET surface area and scanning electron microscope analysis

BC450 had the highest ammonium removal capacity, and was thus selected for further analysis. BET surface areas of digested sludge and BC450 were 1.92 m^2/g and 20.86 m^2/g, respectively. Depolymerization and total char pore volume increase from 0.364 cm^3/g to 0.664 cm^3/g were observed and attributed to the high pyrolysis temperature which caused thermally unstable compounds in biochar to convert to a gaseous state (Li et al., 2016; Lua et al., 2006; Marriott et al., 2016).

As shown in Fig. 2, compared to digested sludge, a rough surface with small holes and pits were observed in BC450. The pyrolysis temperature of 450 °C appears to have softened the sludge material and caused a release of volatile compounds (i.e., hydrocarbons, CO, CO_2, and H_2O) and the crystallization of carbon in the sludge (Zhong et al., 2016; Zielinska and Oleszczuk, 2016). These observations agree with the BET surface analysis results (BC450 *vs.* digested sludge).

3.3.2. Potentiometric titrations

Acid-base titrations indicated that BC450 had measurable proton buffering capacity. Fig. S1 and Table S1 show the excess charge per gram of biochar. There was no difference between forward and reverse pH titrations, indicating that proton adsorption and desorption reactions were reversible. The slope in Fig. S1 represents the rate of ligand deprotonation and buffering capacity at any point for a given pH. The best-fit protonation model invoked three discrete surface functional groups, and their modelled pK_a values of those groups suggest that carboxylic, phenolic, hydroxyl, and lactonic (lactic acid) groups are active in proton adsorption and desorption (Alam et al., 2018) (Table S1). The FTIR data, presented in section 3.2, also support the presence of these functional groups.

3.4. Effect of pH and initial ammonium concentration on ammonium adsorption by BC450

Solution pH and initial ammonium concentration are two important factors in biochar ammonium adsorption. Fig. 3(a) shows the amount of ammonium adsorbed on BC450 after 24 h. The final

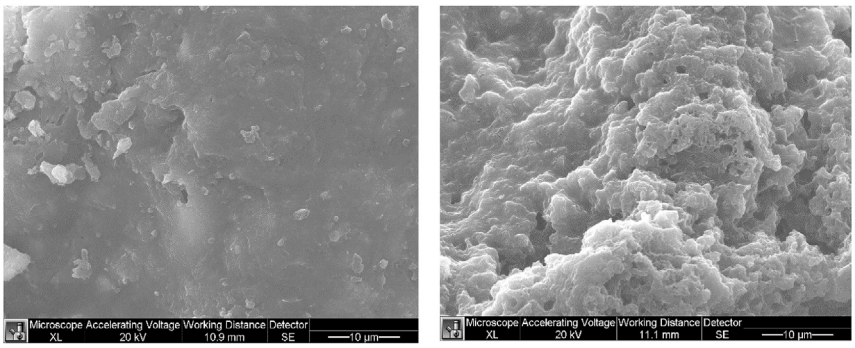

Fig. 2. SEM image of (a) digested sludge and (b) biochar sample BC450.

amount of adsorbed ammonium increased significantly ($p < 0.001$) as the initial pH increased from 2 to 6, and decreased slightly ($p = 0.6$) when pH increased to 8. At acidic conditions, the ammonium removal capacity was low, which is attributed to the strong competition between H^+ and NH_4^+ in the solution for adsorption to biochar surface functional groups. Similar results have been reported by other researchers (Ismail and Hameed, 2014; Kizito et al., 2015; Moreno-Castilla, 2004; Vu et al., 2017). A significant reduction ($p < 0.05$) in ammonium adsorption capacity was observed when pH reached 10, which is due to the effects of pH on the state of ammonium, i.e., it converts to NH_3 (Vu et al., 2017). Table S2 shows the calculated stability constants of ammonium to the three BC450 ligand types. Since the model best fit the ammonium adsorption data by invoking the first two (of three) sites calculated in the protonation model, it is assumed that ammonium mostly adsorbs to carboxyl and phenolic functional groups.

Fig. 3(b) shows the effect of the initial ammonium concentration on ammonium removal by BC450 after 24 h of contact (adsorption equilibrium). NH_4^+ removal efficiencies range between 48% and 58% at lower initial ammonium concentrations (2–10 mg/L), and decreases to <20% ($p < 0.001$) when initial ammonium concentration reached 80 mg/L. This result is plausible since the removal efficiencies of the adsorbate are a function of both the characteristics and concentration of the adsorbate (Eddy, 2014). The Q_e value increased ($p < 0.001$) as the initial ammonium concentration increased until it approximated the adsorption capacity at equilibrium. After the initial NH_4^+ concentration reached 40 mg/L, the value of Q_e increased more slowly ($p = 0.001$). When the initial NH_4^+ concentration reached 80 mg/L, the Q_e value was almost the same as the theoretical adsorption capacity of biochar for ammonium, which was determined by modeling the ammonium adsorption isotherm as described below.

3.5. Adsorption isotherms and kinetics models

Isotherm models were used to define the relationship between adsorbate in liquid and solid (Hameed et al., 2008). The biochar ammonium adsorption capacity was evaluated using the widely applied Langmuir and Freundlich adsorption isotherm models for single solute systems (Fig. 4) (Bashir et al., 2018; Cazetta et al., 2011; Li et al., 2018; Vu et al., 2017, 2018). The Langmuir model is based on the assumption that adsorption occurs in a complete monolayer on a homogenous surface (Kannan and Sundaram, 2001; Wang et al., 2010). The separation factor (R_L) is the essential characteristic of the Langmuir isotherm (Weber and Chakravorti, 1974). Freundlich isotherms are used to describe heterogenous systems and reversible adsorption (Ozcan et al., 2009), and are conceptually a derivation of the Langmuir model where the adsorption energy decreases logarithmically as the fraction of occupied sites (Q/Q_m) increases (Limousin et al., 2007). According to Ayoob et al. (2007), R_L represents the ratio of the remaining adsorption capacity over the total adsorption capacity. The adsorption in the system can be

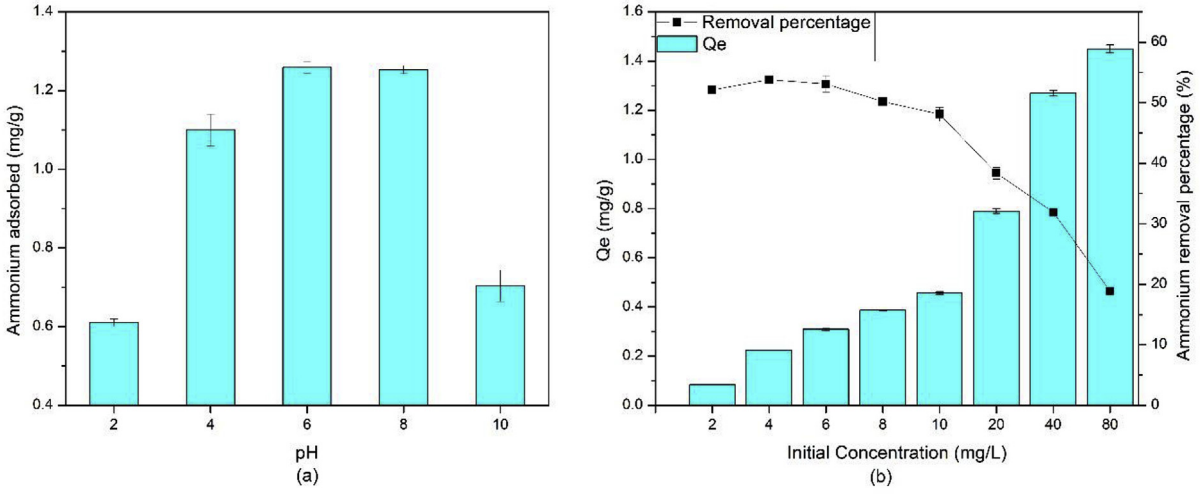

Fig. 3. Ammonium adsorption capacity of BC450 versus (a) initial pH and (b) initial ammonium concentration.

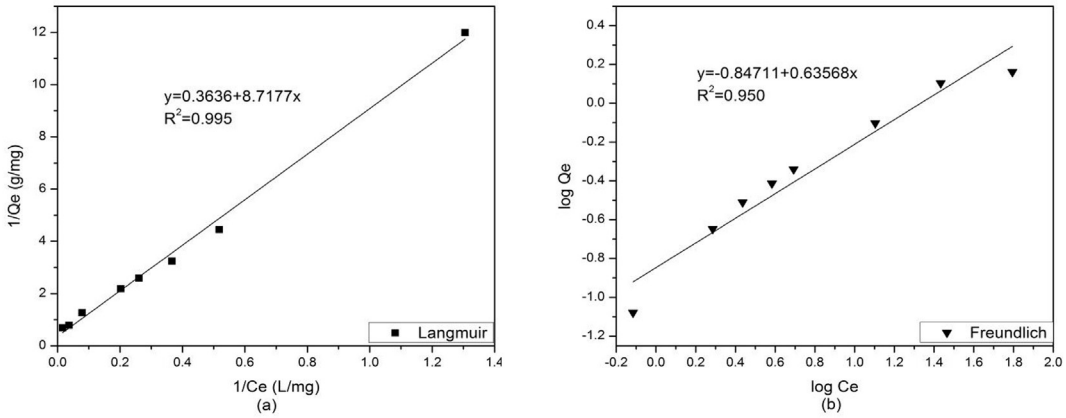

Fig. 4. Isotherm analyses of BC450 ammonia adsorption with (a) the Langmuir model and (b) the Freundlich model.

evaluated using the R_L value, if $0 < R_L < 1$; otherwise, the R_L value cannot be used to evaluate the adsorption (Cazetta et al., 2011). The statistically higher R^2 value of 0.995 of the Langmuir isotherm compared with the 0.950 for the Freundlich model indicates that the Langmuir isotherm fits the experimental data better than does the Freundlich model, and that the adsorption occurred largely in a monolayer on the biochar with a nearly homogenous distribution of binding sites. Further, the R_L value of 0.697 is another indication that adsorption of ammonium from solution onto the digested sludge biochar is favorable.

Kinetics models were used to investigate the reaction dynamics and reaction rates of ammonium adsorption to biochar. The experimental data were utilized to fit pseudo-first order and pseudo-second order models with the kinetics parameters shown in Table S3 and a pseudo-second order model was found to fit better. According to the pseudo-second order model, the theoretical ammonium capacity of BC450 is 1.52 mg/g, which is close to the value observed in the experimental data (1.4 mg/g), indicating the chemisorption may dominate ammonium removal by biochar. The intra-particle diffusion plots in Fig. 5(c) show two-stages in ammonium adsorption by biochar. The first stage corresponded to the adsorption process from 0 to 600 min (t^2 value: 0–25) and

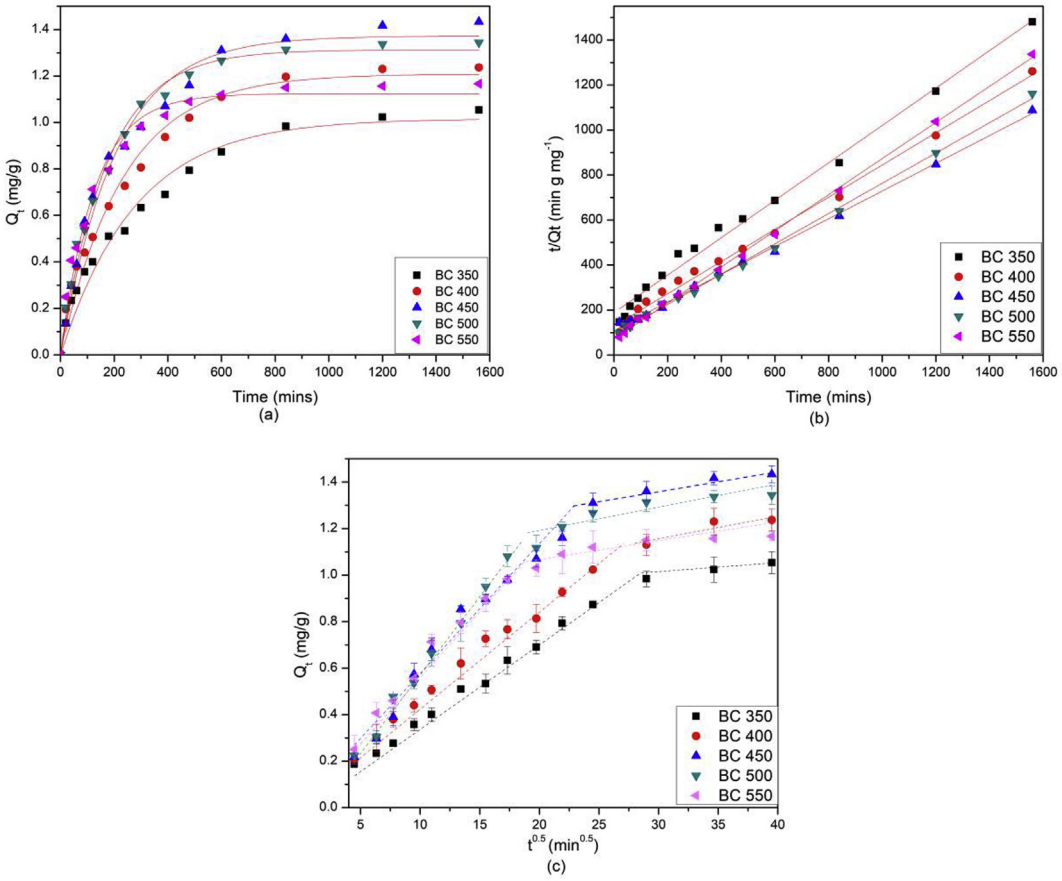

Fig. 5. Biochar ammonium adsorption kinetics using (a) the Lagergren pseudo-first order model, (b) a pseudo-second order model, and (c) intraparticle diffusion.

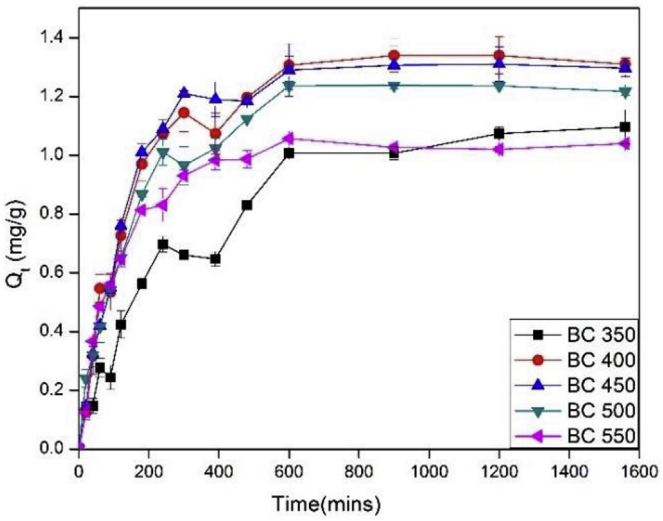

Fig. 6. Removal of ammonium from municipal wastewater by biochars as a function of pyrolysis temperature.

represents the intraparticle diffusion step and the rate-limiting step. In the second stage the adsorption reaches its equivalent point (known as site saturation), that is, the adsorption and desorption speeds are the same and equilibrium is achieved.

3.6. Digested sludge biochar treating municipal wastewater

Digested sludge was pyrolyzed at different temperatures and applied to remove ammonium from municipal wastewater obtained from the GBWWTP (Fig. 6). Before applying the biochar to the municipal wastewater, the wastewater was sterilized to prevent the interference of biological activity with ammonium adsorption. The overall biochar ammonium removal performance from municipal wastewater (Fig. 6) was similar to that in the synthetic ammonium solutions (Fig. 1(b)), yet more fluctuations were observed from the curves when testing the municipal wastewater. This was possibly due to the competition for adsorption or binding sites of biochar from the presence of other contaminants (such as COD, PO_4^{3-} and NO_3^-) in wastewater. Sharp declines in ammonium adsorption were observed in the first 400–600 min for biochars produced at all 5 pyrolysis temperatures (Fig. 1(b)). Based on previous kinetics modeling and isotherm results, those declines may be attributed to limited pore transfer speed and weak interactions (Eddy, 2014). The relatively large surface pore size and volume in digested sludge biochar allows for the adsorption of high molecular weight organic molecules.

Similar results have been previously reported (Wang et al., 2016). Most biochar samples had a lower ammonium adsorption capacity in the municipal wastewater than in the ammonium solution because of interference from other compounds in the municipal wastewater (Wang et al., 2016). Figure 1(b) and Figure 6 indicate that 450 °C was the most effective pyrolysis temperature to produce digested sludge biochar for ammonium adsorption, and future experiments with wastewater ammonium adsorption can benefit by considering this result.

4. Conclusions

In this study, digested sludge was pyrolyzed to improve its ammonium adsorption capacity. Biochar pyrolyzed at 450 °C adsorbed ammonium from aqueous solution and municipal wastewater more efficiently than biochars pyrolyzed at lower and higher temperatures. Indeed, biochar produced at 450 °C achieved a balance between optimum pH and reasonable surface functional group concentrations. The presence of carboxylic and phenolic functional groups in the biochar was confirmed by FTIR and potentiometric titrations. Acidic or pH above 10 conditions limited the digester sludge ammonia removal capacity, and the initial ammonium concentration is positively correlated with Q_e, the equilibrium sorption capacity. The biochar ammonium adsorption from municipal wastewater and aqueous ammonium solution fit a pseudo second-order kinetics model, which suggests that the process was controlled by chemisorption. Langmuir and Freundlich isotherms were used to analyze the relationship between adsorbate and adsorbent at the equilibrium point; the Langmuir model fits the experimental data better than the Freundlich model, which indicates that monolayer adsorption on nearly homogenous binding sites of biochar is the dominant process. We propose, for the first time ever, that digested sludge biochar can be used as a cost-effective, on site method to remove ammonium from municipal wastewater.

Acknowledgement

The authors thank for the financial support from Dr Liu's Natural Sciences and Engineering Research Council of Canada (NSERC) discovery grant and Canada Research Chair program, and technical support from EPCOR Water Services.

Appendix A. Supplementary data

Supplementary data to this article can be found online at https://doi.org/10.1016/j.jclepro.2018.10.268.

References

Alam, M.S., Swaren, L., von Gunten, K., Cossio, M., Bishop, B., Robbins, L.J., Hou, D., Flynn, S.L., Ok, Y.S., Konhauser, K.O., Alessi, D.S., 2018. Application of surface complexation modeling to trace metals uptake by biochar-amended agricultural soils. Appl. Geochem. 88, 103–112.
Ayoob, S., Gupta, A.K., Bhakat, P.B., 2007. Performance evaluation of modified calcined bauxite in the sorptive removal of arsenic(III) from aqueous environment. Colloid. Surface. Physicochem. Eng. Aspect. 293 (1–3), 247–254.
Bashir, S., Rizwan, M.S., Salam, A., Fu, Q.L., Zhu, J., Shaaban, M., Hu, H.Q., 2018. Cadmium immobilization potential of rice straw-derived biochar, zeolite and rock phosphate: extraction techniques and adsorption mechanism. Bull. Environ. Contam. Toxicol. 100 (5), 727–732.
Blanchard, G., Maunaye, M., Martin, G., 1984. Removal of heavy metals from waters by means of natural zeolites. Water Res. 18 (12), 1501–1507.
Bridle, T.R., Pritchard, D., 2004. Energy and Nutrient Recovery from Sewage Sludge via Pyrolysis. Water Science and Technology, pp. 169–175.
Bright, D.A., Healey, N., 2003. Contaminant risks from biosolids land application: contemporary organic contaminant levels in digested sewage sludge from five treatment plants in Greater Vancouver, British Columbia. Environ. Pollut. 126 (1), 39–49.
Carey, D.E., McNamara, P.J., Zitomer, D.H., 2015. Biochar from pyrolysis of biosolids for nutrient adsorption and turfgrass cultivation. Water Environ. Res. 87 (12), 2098–2106.
Cazetta, A.L., Vargas, A.M.M., Nogami, E.M., Kunita, M.H., Guilherme, M.R., Martins, A.C., Silva, T.L., Moraes, J.C.G., Almeida, V.C., 2011. NaOH-activated carbon of high surface area produced from coconut shell: kinetics and equilibrium studies from the methylene blue adsorption. Chem. Eng. J. 174 (1), 117–125.
Chen, X., Jeyaseelan, S., Graham, N., 2002. Physical and chemical properties study of the activated carbon made from sewage sludge. Waste Manag. 22 (7), 755–760.
Eddy, M., 2014. Wastewater Engineering: Treatment and Resource Recovery, fifth ed. McGraw-Hill Education, New York, NY.
Fan, Y., Wang, B., Yuan, S., Wu, X., Chen, J., Wang, L., 2010. Adsorptive removal of chloramphenicol from wastewater by NaOH modified bamboo charcoal. Bioresour. Technol. 101 (19), 7661–7664.
Freundlich, H.M.F., 1906. Over the adsorption in solution. J. Phys. Chem. 57, 385–471.
Gao, F., Xue, Y.W., Deng, P.Y., Cheng, X.R., Yang, K., 2015. Removal of aqueous ammonium by biochars derived from agricultural residuals at different pyrolysis temperatures. Chem. Speciat. Bioavailab. 27 (2), 92–97.
Gao, N.B., Li, J.J., Qi, B.Y., Li, A.M., Duan, Y., Wang, Z., 2014. Thermal analysis and

products distribution of dried sewage sludge pyrolysis. J. Anal. Appl. Pyrol. 105, 43–48.
Hameed, B.H., Tan, I.A.W., Ahmad, A.L., 2008. Adsorption isotherm, kinetic modeling and mechanism of 2,4,6-trichlorophenol on coconut husk-based activated carbon. Chem. Eng. J. 144 (2), 235–244.
Herbelin, A.L.a.J.C.W., 1999. FITEQL 4.0: a Computer Program for Determination of Chemical Equilibrium Constants from Experimental Data. Department of Chemistry. Oregon. Report 99-01.
Hina, K., Hedley, M., Camps-Arbestain, M., Hanly, J., 2015. Comparison of pine bark, biochar and zeolite as sorbents for NH_4^+-N removal from water. Clean. - Soil, Air, Water 43 (1), 86–91.
Ho, Y.S., McKay, G., 1999. Pseudo-second order model for sorption processes. Process Biochem. 34 (5), 451–465.
Hospido, A., Moreira, T., Martín, M., Rigola, M., Feijoo, G., 2005. Environmental evaluation of different treatment processes for sludge from urban wastewater treatments: anaerobic Digestion versus Thermal Processes (10 pp). Int. J. Life Cycle Assess. 10 (5), 336–345.
Hou, J., Huang, L., Yang, Z.M., Zhao, Y.Q., Deng, C.R., Chen, Y.C., Li, X., 2016. Adsorption of ammonium on biochar prepared from giant reed. Environ. Sci. Pollut. Control Ser. 23 (19), 19107–19115.
Inyang, M., Gao, B., Yao, Y., Xue, Y.W., Zimmerman, A.R., Pullammanappallil, P., Cao, X.D., 2012. Removal of heavy metals from aqueous solution by biochars derived from anaerobically digested biomass. Bioresour. Technol. 110, 50–56.
Ismail, Z.Z., Hameed, B.B., 2014. A new application of giant reed waste material for ammonium removal. Int. J. Environ. Stud. 71 (2), 122–138.
Jiang, Y., Raliya, R., Fortner, J.D., Biswas, P., 2016. Graphene oxides in water: correlating morphology and surface chemistry with aggregation behavior. Environ. Sci. Technol. 50 (13), 6964–6973.
Jin, H., Capareda, S., Chang, Z., Gao, J., Xu, Y., Zhang, J., 2014. Biochar pyrolytically produced from municipal solid wastes for aqueous As(V) removal: adsorption property and its improvement with KOH activation. Bioresour. Technol. 169, 622–629.
Jin, J., Li, Y., Zhang, J., Wu, S., Cao, Y., Liang, P., Zhang, J., Wong, M.H., Wang, M., Shan, S., Christie, P., 2016. Influence of pyrolysis temperature on properties and environmental safety of heavy metals in biochars derived from municipal sewage sludge. J. Hazard Mater. 320, 417–426.
Jindarom, C., Meeyoo, V., Kitiyanan, B., Rirksomboon, T., Rangsunvigit, P., 2007. Surface characterization and dye adsorptive capacities of char obtained from pyrolysis/gasification of sewage sludge. Chem. Eng. J. 133 (1–3), 239–246.
Kacan, E., 2016. Optimum BET surface areas for activated carbon produced from textile sewage sludges and its application as dye removal. J. Environ. Manag. 166, 116–123.
Kannan, N., Sundaram, M.M., 2001. Kinetics and mechanism of removal of methylene blue by adsorption on various carbons - a comparative study. Dyes Pigments 51 (1), 25–40.
Kim, H.B., Kim, S.H., Jeon, E.K., Kim, D.H., Tsang, D.C.W., Alessi, D.S., Kwon, E.E., Baek, K., 2018. Effect of dissolved organic carbon from sludge, Rice straw and spent coffee ground biochar on the mobility of arsenic in soil. Sci. Total Environ. 636, 1241–1248.
Kizito, S., Wu, S., Kipkemoi Kirui, W., Lei, M., Lu, Q., Bah, H., Dong, R., 2015. Evaluation of slow pyrolyzed wood and rice husks biochar for adsorption of ammonium nitrogen from piggery manure anaerobic digestate slurry. Sci. Total Environ. 505, 102–112.
Lagergren, S.Y., 1898. Zur theorie der sogenannten adsorption gelöster stoffe. Kungliga Svenska Vetenskapsakademiens, Handlingar 24 (4), 1–39.
Langmuir, I., 1918. The adsorption of gases on plane surfaces of glass, mica and platinum. J. Am. Chem. Soc. 40 (9), 1361–1403.
Li, A., Liu, H.L., Wang, H., Xu, H.B., Jin, L.F., Liu, J.L., Hu, J.H., 2016. Effects of temperature and heating rate on the characteristics of molded bio-char. Bioresources 11 (2), 3259–3274.
Li, L., Liu, Y., 2009. Ammonia removal in electrochemical oxidation: mechanism and pseudo-kinetics. J. Hazard Mater. 161 (2–3), 1010–1016.
Li, S.M., Barreto, V., Li, R.W., Chen, G., Hsieh, Y.P., 2018. Nitrogen retention of biochar derived from different feedstocks at variable pyrolysis temperatures. J. Anal. Appl. Pyrol. 133, 136–146.
Limousin, G., Gaudet, J.P., Charlet, L., Szenknect, S., Barthes, V., Krimissa, M., 2007. Sorption isotherms: a review on physical bases, modeling and measurement. Appl. Geochem. 22 (2), 249–275.
Lin, Y., Wang, D., Wang, T., 2012. Ethanol production from pulp & paper sludge and monosodium glutamate waste liquor by simultaneous saccharification and fermentation in batch condition. Chem. Eng. J. 191, 31–37.
Liu, T.H., Li, Y.H., Du, Q.J., Sun, J.K., Jiao, Y.Q., Yang, G.M., Wang, Z.H., Xia, Y.Z., Zhang, W., Wang, K.L., Zhu, H.W., Wu, D.H., 2012. Adsorption of methylene blue from aqueous solution by graphene. Colloids Surfaces B Biointerfaces 90, 197–203.
Lu, H., Zhang, W., Wang, S., Zhuang, L., Yang, Y., Qiu, R., 2013. Characterization of sewage sludge-derived biochars from different feedstocks and pyrolysis temperatures. J. Anal. Appl. Pyrol. 102, 137–143.
Lua, A.C., Lau, F.Y., Guo, J., 2006. Influence of pyrolysis conditions on pore development of oil-palm-shell activated carbons. J. Anal. Appl. Pyrol. 76 (1–2), 96–102.
Marriott, A.S., Hunt, A.J., Bergstrom, E., Thomas-Oates, J., Clark, J.H., 2016. Effect of rate of pyrolysis on the textural properties of naturally-templated porous carbons from alginic acid. J. Anal. Appl. Pyrol. 121, 62–66.
Mohan, D., Sarswat, A., Ok, Y.S., Pittman, C.U., 2014. Organic and inorganic contaminants removal from water with biochar, a renewable, low cost and sustainable adsorbent - a critical review. Bioresour. Technol. 160, 191–202.
Moreno-Castilla, C., 2004. Adsorption of organic molecules from aqueous solutions on carbon materials. Carbon 42 (1), 83–94.
Nze, K., Xu, S.N., Tang, Y., Mohammed, A., Liu, Y., 2018. Effect of flow rate increase on the performance of a pilot-scale biological nutrient removal reactor. J. Environ. Eng. 144 (5), 04018022.
Ozcan, A.S., Gok, O., Ozcan, A., 2009. Adsorption of lead(II) ions onto 8-hydroxy quinoline-immobilized bentonite. J. Hazard Mater. 161 (1), 499–509.
Paz-Ferreiro, J., Nieto, A., Mendez, A., Askeland, M.P.J., Gasco, G., 2018. Biochar from biosolids pyrolysis: a review. Int. J. Environ. Res. Publ. Health 15 (5), 956.
Peng, C., Zhai, Y.B., Zhu, Y., Xu, B.B., Wang, T.F., Li, C.T., Zeng, G.M., 2016. Production of char from sewage sludge employing hydrothermal carbonization: char properties, combustion behavior and thermal characteristics. Fuel 176, 110–118.
Roque-Malherbe, R., Marquez-Linares, F., Del Valle, W., Thommes, M., 2008. Ammonia adsorption on nanostructured silica materials for hydrogen storage and other applications. J. Nanosci. Nanotechnol. 8 (11), 5993–6002.
Shi, L., Zhang, G., Wei, D., Yan, T., Xue, X.D., Shi, S.S., Wei, Q., 2014. Preparation and utilization of anaerobic granular sludge-based biochar for the adsorption of methylene blue from aqueous solutions. J. Mol. Liq. 198, 334–340.
Shin, J., Choi, E., Jang, E., Hong, S.G., Lee, S., Ravindran, B., 2018. Adsorption characteristics of ammonium nitrogen and plant responses to biochar pellet. Sustainability 10 (5), 1331.
Shinogi, Y., Kanri, Y., 2003. Pyrolysis of plant, animal and human waste: physical and chemical characterization of the pyrolytic products. Bioresour. Technol. 90 (3), 241–247.
Silva, T.L., Ronix, A., Pezoti, O., Souza, L.S., Leandro, P.K.T., Bedin, K.C., Beltrame, K.K., Cazetta, A.L., Almeida, V.C., 2016. Mesoporous activated carbon from industrial laundry sewage sludge: adsorption studies of reactive dye Remazol Brilliant Blue R. Chem. Eng. J. 303, 467–476.
Smith, K.M., Fowler, G.D., Pullket, S., Graham, N.J.D., 2009. Sewage sludge-based adsorbents: a review of their production, properties and use in water treatment applications. Water Res. 43 (10), 2569–2594.
Strezov, V., Evans, T.J., 2009. Thermal processing of paper sludge and characterisation of its pyrolysis products. Waste Manag. 29 (5), 1644–1648.
Stuart, M., Levit, M., JD, 2010. A Literature Review of Effects of Ammonia on Fish. The Nature Conservancy, pp. 1–10.
Veksha, A., McLaughlin, H., Layzell, D.B., Hill, J.M., 2014. Pyrolysis of wood to biochar: increasing yield while maintaining microporosity. Bioresour. Technol. 153, 173–179.
Vithanage, M., Rajapaksha, A.U., Ahmad, M., Uchimiya, M., Dou, X.M., Alessi, D.S., Ok, Y.S., 2015. Mechanisms of antimony adsorption onto soybean stover-derived biochar in aqueous solutions. J. Environ. Manag. 151, 443–449.
Vu, M.T., Chao, H.P., Trinh, T.V., Le, T.T., Lin, C.C., Tran, H.N., 2018. Removal of ammonium from groundwater using NaOH-treated activated carbon derived from corncob wastes: batch and column experiments. J. Clean. Prod. 180, 560–570.
Vu, T.M., Trinh, V.T., Doan, D.P., Van, H.T., Nguyen, T.V., Vigneswaran, S., Ngo, H.H., 2017. Removing ammonium from water using modified corncob-biochar. Sci. Total Environ. 579, 612–619.
Wang, B., Lehmann, J., Hanley, K., Hestrin, R., Enders, A., 2015. Adsorption and desorption of ammonium by maple wood biochar as a function of oxidation and pH. Chemosphere 138, 120–126.
Wang, L., Zhang, J., Zhao, R., Li, Y., Li, C., Zhang, C.L., 2010. Adsorption of Pb(II) on activated carbon prepared from polygonum orientale linn.: kinetics, isotherms, pH, and ionic strength studies. Bioresour. Technol. 101 (15), 5808–5814.
Wang, Y.M., Tian, W.J., Wu, C.L., Bai, J., Zhao, Y.G., 2016. Synthesis of coal cinder balls and its application for COD_{Cr} and ammonia nitrogen removal from aqueous solution. Desalin. Water Treat. 57 (46), 21781–21793.
Weber, T.W., Chakravorti, R.K., 1974. Pore and solid diddusion models for fixed-bed adsorbers. AlChE J. 20 (2), 228–238.
Xu, S.N., Adhikari, D., Huang, R.X., Zhang, H., Tang, Y.Z., Roden, E., Yang, Y., 2016. Biochar-facilitated microbial reduction of hematite. Environ. Sci. Technol. 50 (5), 2389–2395.
Yang, Q., Peng, Y.Z., Liu, X.H., Zeng, W., Mino, T., Satoh, H., 2007. Nitrogen removal via nitrite from municipal wastewater at low temperatures using real-time control to optimize nitrifying communities. Environ. Sci. Technol. 41 (23), 8159–8164.
Yang, X., Igalavithana, A.D., Oh, S.E., Nam, H., Zhang, M., Wang, C.H., Kwon, E.E., Tsang, D.C.W., Ok, Y.S., 2018. Characterization of bioenergy biochar and its utilization for metal/metalloid immobilization in contaminated soil. Sci. Total Environ. 640, 704–713.
Yao, H., Lu, J., Wu, J., Lu, Z.Y., Wilson, P.C., Shen, Y., 2013. Adsorption of fluoroquinolone antibiotics by wastewater sludge biochar: role of the sludge source. Water Air Soil Pollut. 224 (1), 1370.
Yu, L., Zhong, Q., 2006. Preparation of adsorbents made from sewage sludges for adsorption of organic materials from wastewater. J. Hazard Mater. 137 (1), 359–366.
Zhang, H., Voroney, R.P., Price, G.W., 2017. Effects of temperature and activation on biochar chemical properties and their impact on ammonium, nitrate, and phosphate sorption. J. Environ. Qual. 46 (4), 889–896.
Zhang, J.S., Wang, Q.Q., 2016. Sustainable mechanisms of biochar derived from brewers' spent grain and sewage sludge for ammonia-nitrogen capture. J. Clean. Prod. 112, 3927–3934.
Zhong, M., Gao, S.Q., Zhou, Q., Yue, J.R., Ma, F.Y., Xu, G.W., 2016. Characterization of

char from high temperature fluidized bed coal pyrolysis in complex atmospheres. Particuology 25, 59–67.
Zhou, F.S., Wang, H., Fang, S.E., Zhang, W.H., Qiu, R.L., 2015. Pb(II), Cr(VI) and atrazine sorption behavior on sludge-derived biochar: role of humic acids. Environ. Sci. Pollut. Control Ser. 22 (20), 16031–16039.
Zielinska, A., Oleszczuk, P., 2016. Effect of pyrolysis temperatures on freely dissolved polycyclic aromatic hydrocarbon (PAH) concentrations in sewage sludge-derived biochars. Chemosphere 153, 68–74.